


Article

Performance Optimization Design Study of Box-Type Substations Subjected to the Combined Effects of Wind, Snow, and Seismic Loads

Meixing Guo ¹, Mingzhu Fang ², Lingyu Wang ², Jie Hu ^{3,*} and Jin Qi ^{3,*} 

¹ School of Design and Art, Lanzhou University of Technology, No. 287, Lan Gongping Road, Qilihe District, Lanzhou 730050, China; guomx316@163.com

² School of Design, Shanghai Jiao Tong University, No. 800, Dongchuan Road, Minhang District, Shanghai 200240, China; fang_mingzhu@sjtu.edu.cn (M.F.); wanglingyu_025@sjtu.edu.cn (L.W.)

³ School of Mechanical and Power Engineering, Shanghai Jiao Tong University, No. 800, Dongchuan Road, Minhang District, Shanghai 200030, China

* Correspondence: hujie@sjtu.edu.cn (J.H.); jinhuaqj@sjtu.edu.cn (J.Q.); Tel.: +86-13585988686 (J.H.); +86-13817005068 (J.Q.)

Abstract: As a pivotal node in both urban and rural power grids, the box-type substation not only serves the functions of power conversion and distribution but also need to provide structural support and environmental adaptability. However, deficiencies in strength, stiffness, or vibration characteristics may lead to vibration and noise issues, and extreme environmental changes can pose risks of structural damage. This study aims to verify and optimize the seismic resistance and environmental adaptability of box-type substations through finite element simulation methods. Using SOLIDWORKS, a three-dimensional model of the box-type substation was constructed, and static and dynamic analyses were conducted using Ansys Workbench to comprehensively evaluate the dynamic response of the box-type substation under wind, snow loads, and seismic action. Through iterative simulations and a comparison of multiple design solutions, the structural optimization of the substation was achieved. The optimized structure balances strength and stiffness, significantly reducing the weight of the substation body, with the wall thickness reduced by 60%. Additionally, the phenomenon of stress concentration on the side walls was eliminated, ensuring that the equivalent stress is below the material yield strength. This research provides methods and empirical results for enhancing the performance and reliability of box-type substations under seismic conditions, confirming the feasibility of a lightweight design, while ensuring structural safety.

Keywords: box-type substation; finite element simulation; verification of numerical models; seismic performance; structural optimization



Citation: Guo, M.; Fang, M.; Wang, L.; Hu, J.; Qi, J. Performance Optimization Design Study of Box-Type Substations Subjected to the Combined Effects of Wind, Snow, and Seismic Loads. *Appl. Sci.* **2024**, *14*, 3958. <https://doi.org/10.3390/app14103958>

Academic Editor: Fernando Rocha

Received: 26 March 2024

Revised: 1 May 2024

Accepted: 3 May 2024

Published: 7 May 2024



Copyright: © 2024 by the authors. Licensee MDPI, Basel, Switzerland. This article is an open access article distributed under the terms and conditions of the Creative Commons Attribution (CC BY) license (<https://creativecommons.org/licenses/by/4.0/>).

1. Introduction

As a core component of the national infrastructure, the power system plays a crucial role in the construction and renovation of urban and rural power grids. Against the backdrop of rapid economic development and a continuous growth in power demand, the efficiency and reliability of power supply are particularly important [1]. Box-type substations, characterized by their compact structure, small footprint, and unmanned operation features, have been widely used in modern power systems. By integrating high-voltage switchgear, distribution transformers, and low-voltage distribution devices, box-type substations provide a flexible and efficient power supply solution for the grid.

However, the structural design of box-type substations is a key determinant of their quality and service life. Once a box-type substation malfunctions, it can have significant impacts on the urban and even national power supply, thereby adversely affecting the national economy. Therefore, conducting an in-depth simulation analysis and research on the operational status and design performance of box-type substations in extreme

natural environments, and proposing corresponding engineering recommendations and design measures to ensure the structural safety and reliability of box-type substations, is of paramount importance.

In recent years, domestic and foreign scholars have conducted a series of studies on the resistance performance of box-type substations under extreme conditions such as typhoons, snowstorms, and earthquakes. In seismic research on building structures and electrical equipment, the static analysis method, response spectrum analysis method, and time-history analysis method are commonly employed [2]. Yu Jianjun et al. [3] designed a box-type substation typhoon-resistance test device and its test procedures, conducted a test analysis of the box-type substation's typhoon resistance capability, and proposed key designs and methods to enhance its typhoon resistance capability. Process improvement verified the reliability of the optimized design solution. Zhou Xuanyi et al. [4] proposed an equivalent static wind load method suitable for multi-response and determined that wind load is one of the important loads in the design of long-span roof structures. Chen Yong et al. [5] conducted a finite element analysis on a 110 kV box-type substation under seismic strong wind conditions, verifying its safety. They extended this analysis method to the areas of substation design and force verification safety, which can provide certain guidance for similar work. Jiang Jiayin et al. [6] invented a vertical box-type substation with shock absorption, focusing on the impact of vibration on substations. However, there are relatively few patents related to snow and wind prevention, as well as earthquake conditions. Temel Türker et al. [7] employed experimental and theoretical analysis methods to compare dynamic characteristics, such as the natural frequencies of steel frame structures with and without supports. They proposed that, during the study of structural seismic performance, the static and dynamic characteristics of the structure should be checked first. According to the research of Aiello G et al. [8], earthquakes can cause structural oscillation or damage, and their acceleration effects can exacerbate resonance. Therefore, when designing structures for seismic resistance, it is necessary to evaluate their modal results and ensure that their seismic performance is not affected by resonance.

These studies, through experimental and theoretical analysis, not only validate the structural safety, but also offer valuable insights for enhancing the design and seismic resistance, of box-type substations. While these studies provide crucial theoretical and experimental evidence for understanding the performance of box-type substations under individual extreme conditions, in real-world scenarios, box-type substations often need to withstand the combined effects of multiple loads such as wind, snow, and earthquakes. This places higher demands on the design of box-type substations, requiring consideration not only of their seismic performance but also an assessment of their performance under combined loading conditions.

Given the limitations of the existing research, this study employs finite element simulation methods, integrating static and dynamic analyses, to systematically investigate the performance of box-type substations under extreme wind, snow, and seismic loads, exploring structural optimization strategies. Firstly, the seismic response spectrum analysis method [9] used in this study calculates the structure's frequency-domain response under seismic actions, combined with its dynamic characteristics, to evaluate its response to seismic loads. It involves determining seismic inputs, calculating seismic response spectra, obtaining the structure's natural vibration modes, matching the seismic response spectrum with the structural modes, computing structural responses, and ultimately assessing structural safety. This method, considering both structural and ground dynamic characteristics, is accurate and widely applied in assessing the seismic performance of power facilities [10]. Secondly, through simulation iterations and comparative analyses, an optimized design solution balancing structural strength and stiffness is proposed. This solution not only reduces the weight and thickness of the enclosure but also ensures that the equivalent stress is below the material's yield strength.

The findings of this study not only provide scientific evidence and practical demonstrations for enhancing the seismic performance and reliability of box-type substations

but also demonstrate the feasibility of a lightweight design in ensuring structural safety, offering valuable theoretical and practical guidance for similar power facility designs and emergency management.

2. Finite Element Model of Box-Type Substation

2.1. Product Model

Based on the design specifications and structural parameters of the box-type substation, corresponding three-dimensional models were constructed. In the model, the high-voltage chamber and low-voltage chamber are arranged internally in sequence, with the outer shell equipped with three maintenance-friendly doors. The box design includes inspection doors, air intakes, and fixed exhaust vents, with the top adopting a sloped design to optimize structural strength and aerodynamic performance. Considering the volume and structural complexity of the box-type substation, this study focuses on simulating the framework structure of the box body, with dimensions of length \times width \times height = 3800 \times 1500 \times 2400 mm.

Prior to conducting a simulation analysis in ANSYS (2022 R1) [11], the model was appropriately simplified to avoid a data-processing overload caused by minor features. This simplification ensures a more concise analysis and objective data, facilitating computations without compromising the analysis results [12]. The simplification steps are as follows: (1) neglecting the influence of the oil tank and heat sink on the seismic performance of the box-type substation; (2) ignoring thinner steel plates inside the box; and (3) stress induced by earthquakes is fully borne by the frame structure. Additionally, structures with a minimal impact on the analysis, such as the fan blades of the inlet and outlet vents, transition fillets, non-critical stiffeners, and small holes, were eliminated. Moreover, bolt connections were treated as integral units. These adjustments have a minimal impact on the finite element analysis results, while preserving the model's primary mechanical performance. The simplified box-type substation model is depicted in Figure 1.

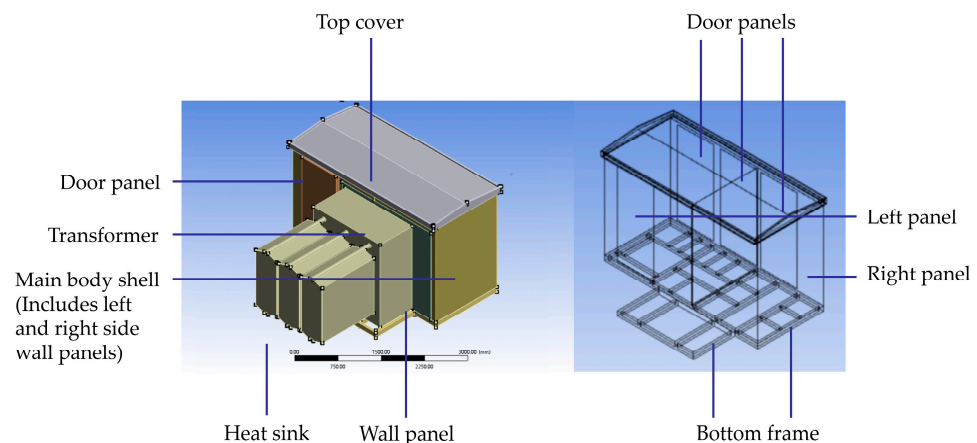


Figure 1. Box-type substation model and simplified model.

2.2. Material Model

The self-weight load is evenly distributed on the entire box-type substation structure, including the bottom frame support structure. The location of static loads and how they are applied to the structure is shown in Figure 2. This model consists of two main materials, namely Q235 steel (GB/T 700-2006) and ST12 steel (GB/T 5213-2019). Q235 is used for the bottom frame, main body shell, and heat sink, while ST12 is used for the outer wall panels, door panels, peripheral structures, and bottom plate. Table 1 lists the key mechanical properties of these two materials, including density, elastic modulus, Poisson's ratio, yield strength, and ultimate strength, providing fundamental data for subsequent structural analysis. In this study, the mechanical properties of Q235 steel and ST12 steel are determined according to their respective standard specifications. Firstly, the mechanical properties of Q235 steel are referenced from the Chinese National Standard GB/T 700 "Carbon Structural Steels" [13].

Secondly, the mechanical properties of ST12 steel are referenced from the Chinese National Standard GB/T 5213-2019 “Cold-rolled Low Carbon Steel Sheet and Strip” [14]. Both of these references provide reliable support for the material properties in question.

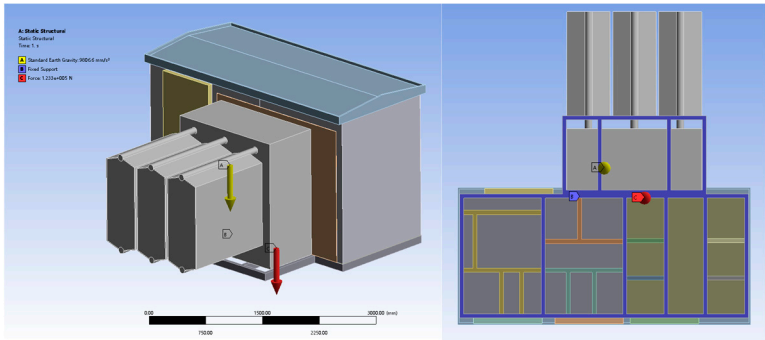


Figure 2. Static loads distribution.

Table 1. Mechanical properties.

Material	Density (Kg/m)	Modulus of Elasticity (GPa)	Poisson’s Ratio	Yield Strength (MPa)
Q235	7850	210	0.3	252
ST12	7800	205	0.32	280

2.3. Load and Boundary Condition Analysis

2.3.1. Static Load

The static load primarily considers the self-weight of the box-type substation, including the weight of all components such as the high-voltage chamber, low-voltage chamber, transformer, and heat sink. Table 2 presents the weights of each structure, totaling approximately 123,300 N. The self-weight load is evenly distributed on the entire box-type substation structure, including the bottom frame support structure. The location of static loads and how they are applied to the structure is shown in Figure 2. In addition, the wind load and snow load in this study will also be applied as static loads along the outer surface of the box-type substation. These loads will produce pressure and suction on the side wall panels and roof of the structure, affecting the lateral stability of the structure. The load distribution is shown in Figure 3.

Table 2. Each structure’s weight.

High-Voltage Chamber	Low-Voltage Chamber	Transformer	Heat Sink
20,000 N	20,000 N	7840 N	75,460 N

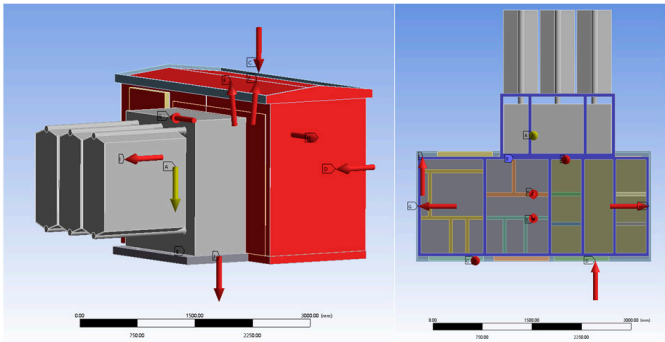


Figure 3. Boundary conditions setting.

2.3.2. Dynamic Load

The dynamic loads in this study mainly come from external factors, here referred to as seismic loads. In this study, seismic loads are simulated through seismic wave response spectra. The load is dynamic and applied horizontally along the base of the box-type substation. Seismic forces act in all three dimensions of a structure (X, Y, Z axes) but primarily in the two most dominant horizontal directions (usually the X and Y axes). This simulates the lateral and longitudinal seismic wave effects in actual earthquakes. In the numerical model, seismic loads are distributed throughout the structure through a mass matrix.

The seismic performance of the box-type substation under a six-degree earthquake is analyzed through static, modal, and response spectrum analyses. Initially, the steady-state static module applies loads to the computational model for structural analysis. Following the static analysis, the results are utilized in a prestressed modal analysis to calculate the natural frequencies and corresponding modes, which consider the preloading effects on the deformation assessment at these frequencies. Finally, the results from static and modal analyses are transferred to the response spectrum module to accomplish the structural response spectrum analysis. The inter-transfer process of the response spectrum analysis module is illustrated in Figure 4.

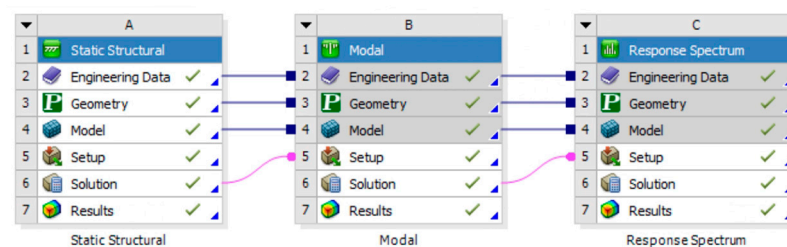


Figure 4. Response spectrum multi-system analysis interface.

2.3.3. Boundary Conditions

Correctly setting the boundary conditions is crucial to ensuring the accuracy of the analysis results. In this study, the base frame of the box-type substation was set to a fixed state to simulate its actual connection to the foundation. Table 3 provides an explanation of the load and constraint conditions used to analyze the seismic performance of the box-type substation. The boundary conditions setting is shown in Figure 4.

Table 3. Boundary conditions analysis.

Condition	Load Conditions	Constraint Conditions
Seismic condition	Apply corresponding seismic acceleration spectra to different directions of the model (X, Y, Z, X + Z, Y + Z) to simulate the excitation experienced by the structure during earthquakes.	The bottom frame of the box-type substation is set to fixed, constraining the material properties of various structures within the box-type substation.
Wind and snow conditions	Apply varying wind pressures to different parts of the model.	

2.3.4. Mesh Model

In the numerical model, the size of the generated mesh affects the accuracy of the simulation solution [15]. To ensure the quality of mesh partitioning and avoid the problem of excessive computational load, Ansys's fully automatic tetrahedral mesh-partitioning method was adopted. To maintain computational accuracy, while ensuring a moderate computational load, the mesh size was set to 50 mm and a gradual-smoothing transition method was employed. According to the mesh-partitioning results, the number of nodes is 785,346, the number of elements is 389,363, and the average mesh quality is 0.34531, indicating a good mesh quality that meets the requirements of the simulation analysis.

Among them, the Jacobian Ratio (Corner Nodes) is 0.98378, and Jacobian Ratio (Gauss Points) is 0.99147. The closer these two values are to 1, the better the mesh quality. Secondly, the Aspect Ratio value is 1.1209, which is greater than 1, indicating that the quality is good. The model diagram obtained after dividing the mesh is shown in Figure 5.

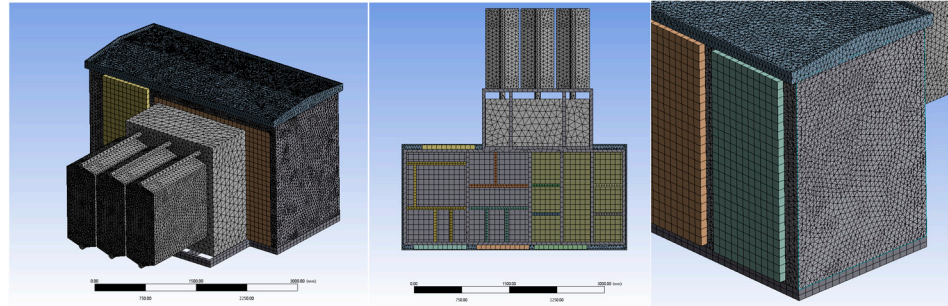


Figure 5. Box grid model diagram of box-type substation.

3. Modal Analysis

The dynamic characteristics of mechanical structures mainly depend on their modal parameters, such as natural frequencies and mode shapes [16]. Modal analysis, which determines the vibration properties of the structure, serves as the foundation for simulating seismic conditions for box-type substations.

3.1. Steady-State Static Analysis Module

Static analysis forms the foundation of structural investigation, focusing on the structural response to static loads and assessing stiffness and load-bearing capacity [17]. The static load generated by the self-weight of the box-type substation initiates the initial stresses, which are crucial in the analysis. To evaluate the enclosure's vibration characteristics, a free modal analysis is initially conducted. In the steady-state static analysis, considering the weight of electrical equipment inside the enclosure, the equipment weight is equivalently applied to the surface of the enclosure's base frame. Additionally, fixed constraints are applied to the base frame of the substation enclosure, along with a vertical downward gravitational acceleration. Upon completion of the calculation, the deformation and stress cloud map of the substation enclosure's frame structure are obtained, as depicted in Figure 6. The results indicate that the maximum total deformation is 0.38246 mm, located at the center of the top cover, with other significant deformations concentrated at the bottom of the high- and low-voltage chambers. The maximum stress is 8.3121 MPa, primarily distributed over the main body of the box-type substation, meeting structural design requirements.

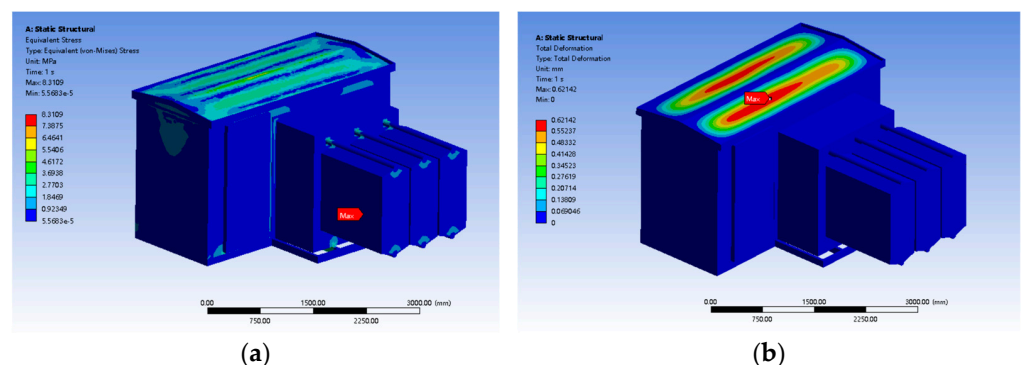


Figure 6. Static structural stress deformation diagram of box frame: (a) static structural stress; (b) static structural deformation.

3.2. Modal Module Analysis

Before conducting a response spectrum analysis, a modal analysis is required for the box-type substation structure to obtain its stiffness characteristics [18]. The relationship between the natural frequency and the reciprocal of the vibration period aids in avoiding resonance damage, by ensuring that the structural vibration period does not coincide with the main vibration period of the earthquake. In modal analysis, low-order and high-order modes exhibit different characteristics. Due to the smaller computational burden and better seismic response of low-order modes, this study employs low-order modes to investigate the dynamic response characteristics of seismic events. The computed results of the first 10 natural frequencies of the enclosure frame are presented in Table 4.

Table 4. The first 15 natural frequencies of the analyzed structure.

Modal Number	Natural Frequency (Hz)
1	7.3331
2	9.4574
3	13.096
4	16.697
5	17.491
6	21.812
7	21.86
8	21.883
9	22.743
10	23.816

The calculation results of the first 10 natural frequencies of the structure are shown in Table 4. The bar graph in Figure 7 shows the change in frequency. Figure 8 lists the simulation cloud diagrams of the total deformation of the box-type substation under the first six modals, showing the characteristic shape of its structure.



Figure 7. The first 10 frequencies.

The frequency range with the highest occurrence probability of seismic waves is between 1 and 10 Hz. As shown in Table 4, it can be seen that, of the first 10 natural frequencies of the prefabricated substation, except for the first and second orders, the other natural frequencies are outside the frequency range where seismic waves occur most often; then, the box-type substation will not resonate with seismic waves [19].

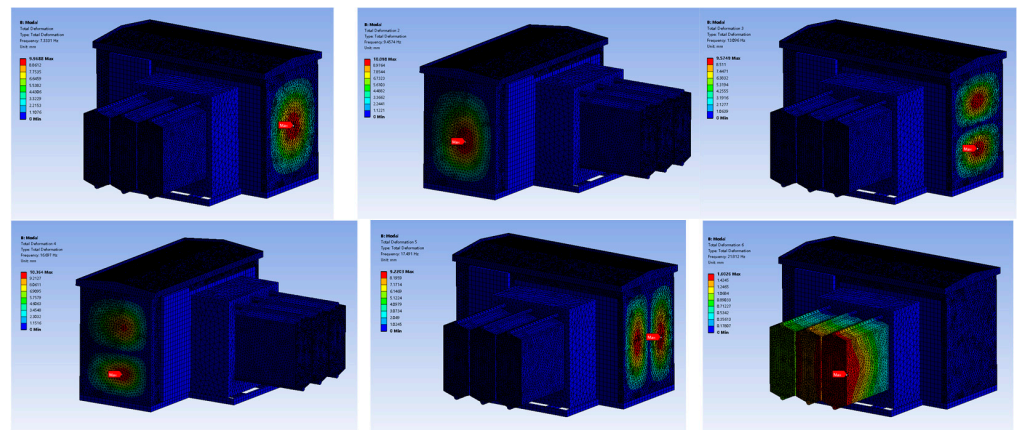


Figure 8. The first six modals of total deformation simulation cloud charts.

3.3. Response Spectrum Module Analysis

In this study, seismic parameters from Lushan County, Ya'an City, Sichuan Province, as delineated in the “Seismic Ground Motion Parameter Zonation Map of China” [20], were selected. The seismic performance of the box-type substation was investigated using the acceleration response spectrum method. The characteristic period T_g was 0.4 s, and the maximum horizontal seismic coefficient α_{max} was 0.15. Using MATLAB, a set of 20 seismic impact coefficient points were derived, based on the generation of a seismic response spectrum and acceleration response spectrum for a sixth-level seismic wave. The corresponding parameters for the acceleration response spectrum were obtained utilizing the seismic response curve, as depicted in Figure 9 and Table 5. These parameter values serve as a scientifically rational basis for the seismic design in the simulation modeling.

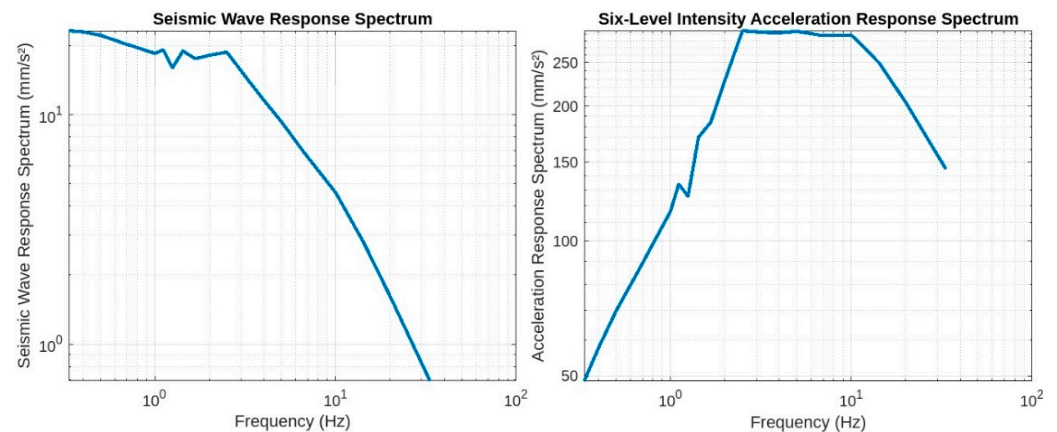
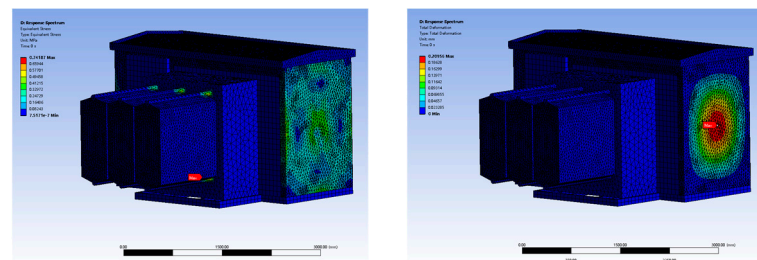
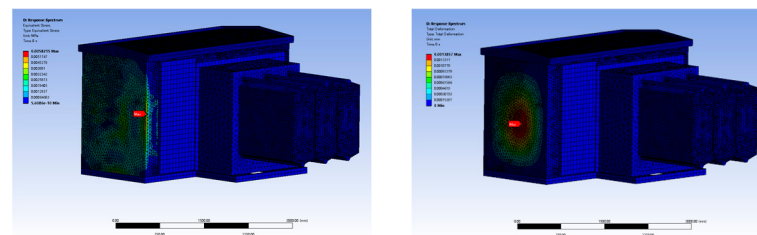
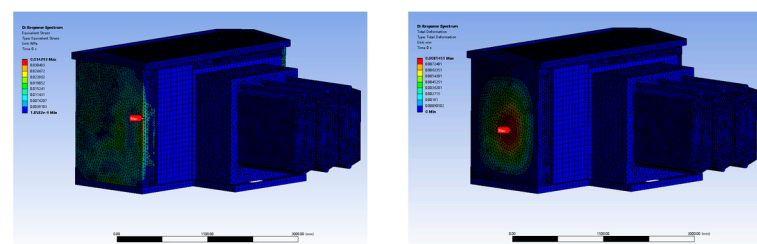


Figure 9. Level sixth seismic wave response spectrum and acceleration response spectrum.

Through the response spectrum module of ANSYS Workbench, the seismic acceleration response of the box structure in different directions was examined, further analyzing the maximum deformation and stress of the box. The simulation results are depicted in Figures 10–14. Observing the simulated data obtained from different seismic wave directions, as shown in Table 6, it is evident that the box exhibits maximum deformation and stress in the X and XZ directions, while the deformation and stress in the Y and Z directions are relatively smaller, suggesting a potentially better stability and seismic resistance in these directions. Considering the simulation results from different directions, the maximum stress values in the structure of the box-type substation are all below the allowable stress of the materials, thus meeting the seismic design requirements under a sixth-level seismic intensity.

Table 5. Acceleration response spectrum parameters.

Modal Number	Natural Frequency (Hz)
0.333	48.675
0.400	57.765
0.500	69.81
0.667	86.085
1.000	116.44
1.111	134.01
1.250	125.93
1.429	170.53
1.667	183.96
2.000	228.47
2.500	294.78
3.333	292.13
4.000	291.58
5.000	293.87
6.667	288.12
10.000	288.87
11.111	276.38
14.286	249.48
20.000	203.91
33.333	144.76

**(a)** X-direction stress response**(b)** X-direction deformation response**Figure 10.** X-direction stress and deformation of box-type substation under earthquake conditions.**(a)** Y-direction stress response**(b)** Y-direction deformation response**Figure 11.** Y-direction stress and deformation of box-type substation under earthquake conditions.**(a)** Z-direction stress response**(b)** Z-direction deformation response**Figure 12.** Z-direction stress and deformation of box-type substation under earthquake conditions.

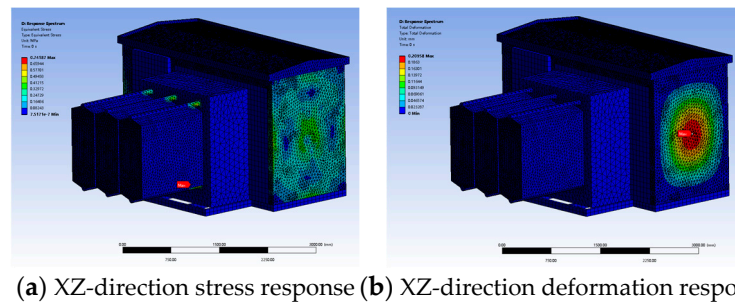


Figure 13. XZ-direction stress and deformation of box-type substation under earthquake conditions.

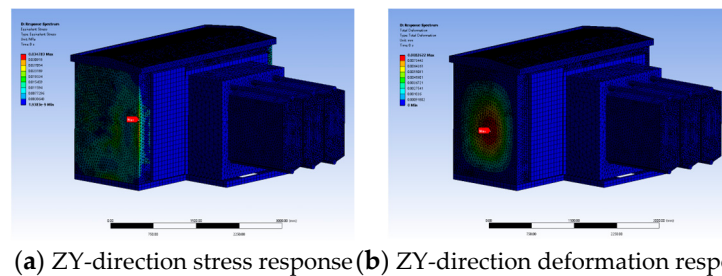


Figure 14. ZY-direction stress and deformation of box-type substation under earthquake conditions.

Table 6. Simulation results for different seismic wave directions.

Response	X	Y	Z	XZ	ZY
Von Mises Stress (MPa)	0.74187	0.0058215	0.034293	0.74187	0.034783
Total Deformation (mm)	0.20956	0.0013857	0.0081451	0.20958	0.0082622

4. Simulation Conditions

4.1. Single Wind and Snow Condition

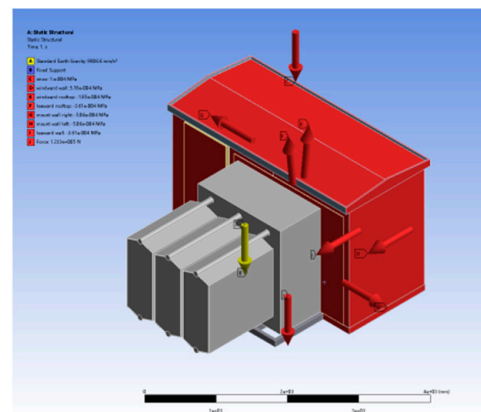
In the study of wind and snow conditions, wind and snow loads are considered as the primary factors, while excluding the effects of thermal stress caused by temperature variations and ash accumulation loads. Additionally, human factors and other uncontrollable variables affecting the structure, such as potential damage during transportation and installation processes, are disregarded.

Initially, static simulations were conducted to assess various thickness configurations, with the aim of selecting an optimal wall thickness scheme. Using a baseline thickness of 2.5 mm and setting a standard step size of 0.5 mm for thickness adjustment, the thickness was incrementally increased to 3 mm to evaluate the specific impact of thickness augmentation on structural performance. Similarly, the thickness was decreased step by step to 2.0 mm, 1.5 mm, 1.0 mm, and 0.5 mm for a comparative analysis. This incremental adjustment method facilitates a detailed observation of the effect of thickness variation on structural stress and strain, providing a scientific basis for determining the optimal thickness. The simulation results are presented in Table 7. A comparative analysis revealed that the stress levels for thicknesses of 1.0 mm, 0.5 mm, and 0.25 mm exceeded the material's yield strength, indicating insufficient structural safety, thus excluding them from subsequent combined load simulations. Additionally, the 2.0 mm- and 1.5 mm-thickness schemes, although approaching the material's yield strength, remained within the safety range, making them ideal candidates for further simulation studies.

Table 7. The simulation results for different wall thicknesses.

Wall Thickness	Maximum Stress (MPa)	Maximum Deformation (mm)	Maximum Strain
3.0	32.876	10.474	0.00015834
2.5	44.019	16.288	0.0002098
2.0	256.68	37.248	0.0012524
1.5	250.47	70.037	0.0013156
1.0	312.8	30.621	0.0015379
0.5	353.96	43.191	0.0020875
0.25	651.07	164.72	0.0082567

Next, after selecting three thickness schemes, considering the extreme wind and snow conditions that inland and coastal regions may encounter, the structural design of the box-type substation in this study needs to withstand wind speeds of level 10 and snow loads of 40–50 cm. The loading conditions are illustrated in Figure 15, where wind load refers to the force exerted on the box-type substation by the wind, and snow load refers to the weight of snow borne by the box-type substation. The formula for wind pressure calculation is $P = 0.613 V^2$, where P is the wind pressure and V is the wind speed. The maximum snow load calculation formula is $w = \rho h$, where w is the snow load, ρ is the density of snow, and h is the depth of snow, assuming a maximum snow depth of 50 mm. After calculation, the maximum wind pressure is 494.42 KPa, and the maximum snow load is 0.98 KN/m². The basic wind pressure is 0.7225. Based on the data mentioned above, the wind and snow loads applied to the windward and leeward walls, as well as the roof of the box-type substation, are derived and presented in Table 8. The stress and deformation results of the box-type substation under the combined action of wind and snow loads are obtained through simulation, as depicted in Figure 16.

**Figure 15.** Boundary condition setting for snow resistance performance analysis.**Table 8.** Box-type substation enclosure wind load standard table (KN/m²).

Load Name	Applied Force Location	Load Magnitude
Standard earth gravity	All objects	9.8 kg·m/s ²
Snow	Windward and leeward roof	1×10^{-4} MPa
Windward wall	Windward wall	5.78×10^{-4} MPa
Leeward wall	Leeward wall	3.61×10^{-4} MPa
Mount wall left/right	Mount wall	-5.06×10^{-4} MPa
Windward rooftop	Windward roof	-1.85×10^{-4} MPa
Leeward rooftop	Leeward roof	-3.61×10^{-4} MPa

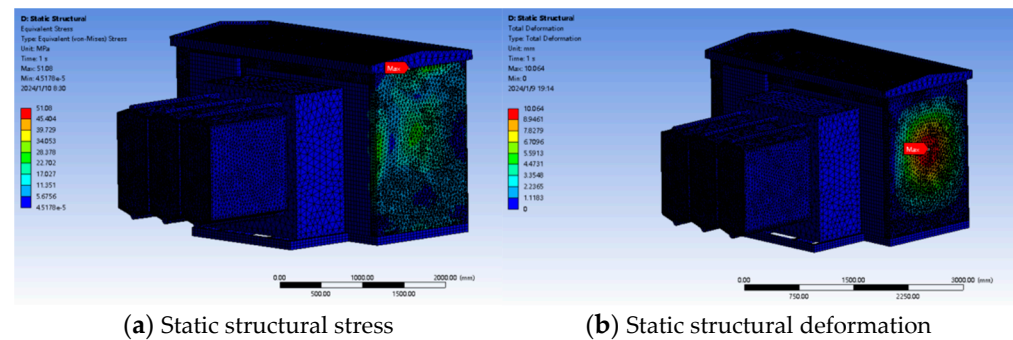


Figure 16. Wind and snow load stress deformation value of the box.

Under the combined action of the wind and snow loads, the maximum stress in the box-type substation structure occurs at the edge of the side wall panel, with a maximum stress of 34.413 MPa, which is below the allowable stress of the material. The maximum deformation of the box-type substation structure is observed at the midpoint of the side wall panels, with a maximum deformation of 7.7699 mm, meeting strength requirements under 10-level wind force.

4.2. Combined Wind, Snow, and Seismic Conditions

Building upon the simulation of individual wind and snow conditions, the next step involves introducing seismic conditions. The key to the integrated simulation study lies in identifying and reinforcing potential weak points in the structure. By applying the seismic wave acceleration power spectrum in the simulation environment, as illustrated in Figure 17, successful simulation results under combined conditions were obtained. This lays the foundation for further optimization proposals.

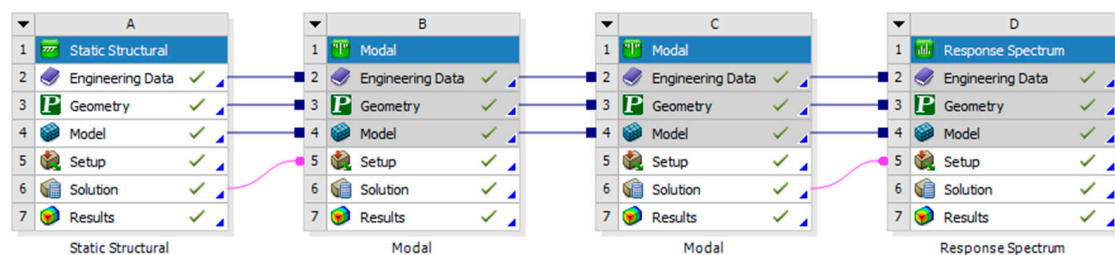


Figure 17. The module connection for the combined wind, snow, and seismic conditions.

In the results of the modal analysis of the first ten modes, it was found that the maximum deformation was concentrated at the side wall position in seven modes. This finding indicates the necessity for optimizing the internal structure of the side wall.

4.2.1. Combined Simulation of Three Wall Thicknesses

During the integrated simulation, errors were encountered in the software environment for the 2.0 mm and 1.5 mm wall thicknesses of the box-type substation. To address this issue, separate mesh divisions were performed for the side wall panels of the substation, with the mesh size reduced from 80 mm to 40 mm, resulting in a successful grid creation. The integrated simulation encompassed the following key steps:

1. Modal analysis focusing on the vibration characteristics of the box-type substation and computing the first 10 mode shapes.
2. Assessment of total deformation for the first 10 modes after applying fixed constraints.
3. Results of response spectrum analysis, including total deformation and equivalent stress.

Figures 18–22 present the stress and deformation results for a 2.5 mm wall thickness. Table 9 displays the deformation and stress performance of the structure under different seismic wave directions for various wall thicknesses. Based on the contour plots of these

three thickness schemes, it is evident that the maximum deformation occurs at the central position of the side walls of the box-type substation, with stress concentrations observed at the edges of the side walls. This finding highlights critical weaknesses in the structural design of the box-type substation, suggesting potential for improving overall stability and safety through structural optimization. Consequently, subsequent optimization strategies will prioritize the side wall positions, to mitigate stress concentrations and reduce the deformation induced by seismic events.

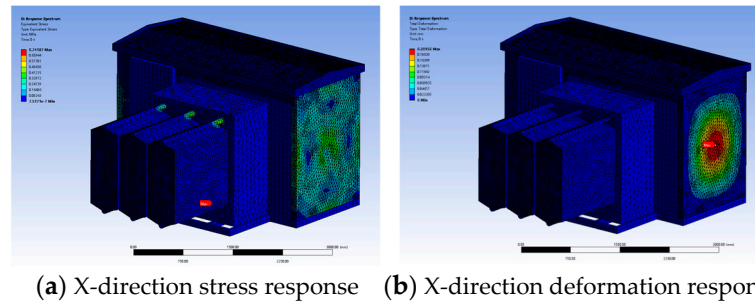


Figure 18. X-direction stress and deformation of box-type substation under combined operating conditions.

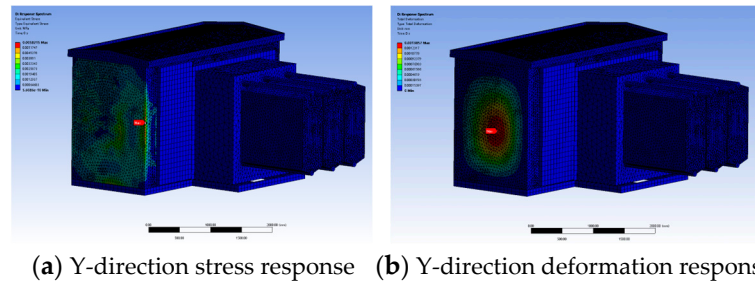


Figure 19. Y-direction stress and deformation of box-type substation under combined operating conditions.

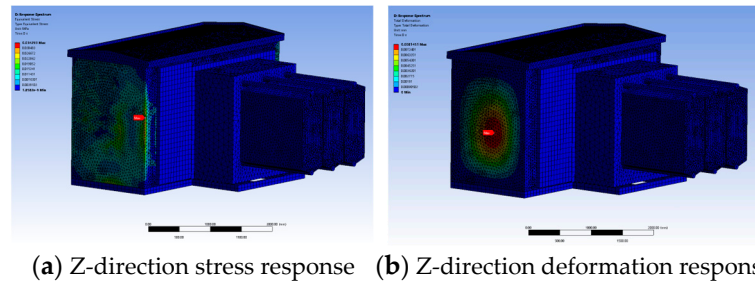


Figure 20. Z-direction stress and deformation of box-type substation under combined operating conditions.

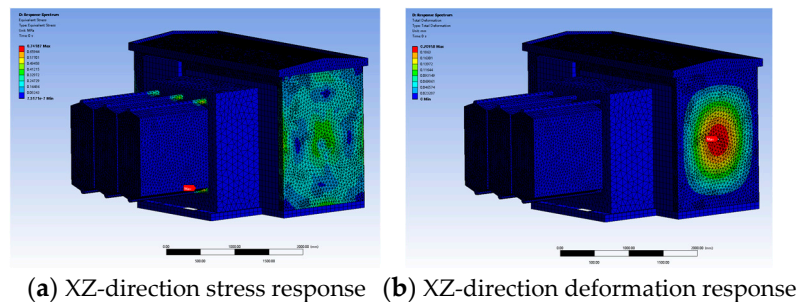


Figure 21. XZ-direction stress and deformation of box-type substation under combined operating conditions.

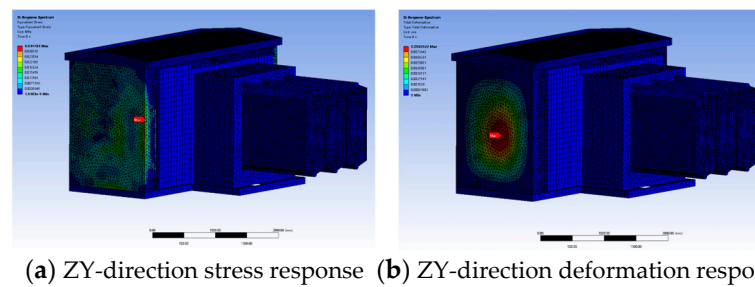


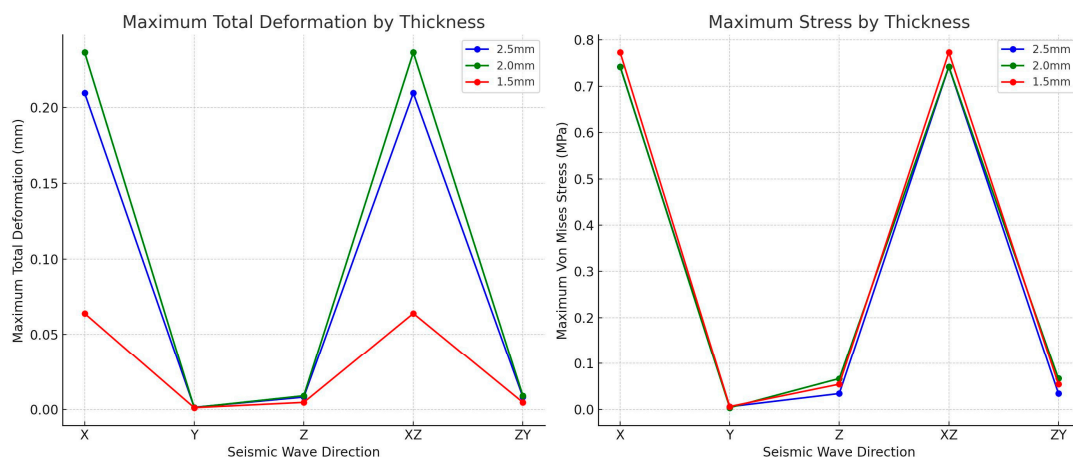
Figure 22. ZY-direction stress and deformation of box-type substation under combined operating conditions.

Table 9. The combined simulation results for the three thicknesses.

Thicknesses	Response	X	Y	Z	XZ	ZY
2.5 mm	Von Mises Stress (MPa)	0.74187	0.0058215	0.034293	0.74187	0.034783
	Total Deformation (mm)	0.20956	0.0013857	0.0081451	0.20958	0.0082622
2.0 mm	Von Mises Stress (MPa)	0.74192	0.0036284	0.066942	0.74192	0.06704
	Total Deformation (mm)	0.23642	0.0012021	0.0090749	0.23642	0.0091109
1.5 mm	Von Mises Stress (MPa)	0.77286	0.0061081	0.054647	0.77286	0.054655
	Total Deformation (mm)	0.06401	0.001135	0.0046594	0.064027	0.0046597

4.2.2. Analysis and Optimization Suggestions

Based on the data from Table 9, graphs depicting the total deformation and stress variations for the three different thicknesses in various directions are plotted in Figure 23. Here, the horizontal axis represents the direction of seismic waves, the vertical axis on the left graph represents the maximum deformation, and the one on the right graph represents the maximum stress. Each line represents a different side wall thickness, distinguished by different colors, with blue indicating 2.5 mm, green indicating 2 mm, and red indicating 1.5 mm for the box-type substation.



(a) Maximum deformation for three thicknesses **(b)** Maximum stress for three thicknesses

Figure 23. The total deformation and stress variation for the three different thicknesses under different directions of seismic waves.

Figure 24 illustrates the total deformation and stress variation for the three thicknesses in the X+Y+Z direction. Combining Figures 23 and 24, the following conclusions can be drawn: (1) Deformation Analysis: The 2.5 mm wall thickness shows the largest deformation in the X direction and the XZ combination direction. The deformation of the 2.0 mm wall thickness in the Y direction and the ZY combination direction is slightly less than that of 2.5 mm, but in the X+Y+Z combination direction. The largest deformation is

0.23642 mm. In contrast, the total deformation of the 1.5 mm wall thickness in all directions remains at a relatively low level, especially in the X+Y+Z combined direction, where its deformation is much lower than the other two thicknesses, which reflects that a thinner wall thickness is superior in maintaining the shape of the structure. Even under the multi-directional action of seismic waves, the 1.5 mm thick structure can better maintain its original shape and reduce damage caused by deformation. (2) Stress Analysis: The stresses in the Y direction and ZY combined direction for the three wall thicknesses are significantly higher than in the other directions, which indicates that the material is more sensitive to seismic waves in these directions. According to the data in Table 9, we observe that the stress values and deformations of the 1.5 mm wall thickness in all single and combined directions are relatively uniform. Although its stress in the YZ combined direction is slightly higher (0.77286 MPa), this difference is very small. Small and without extreme peaks, its response to seismic waves is relatively uniform, and this also indicates that a thinner wall thickness can provide a sufficient anti-deformation performance, without sacrificing too much strength.

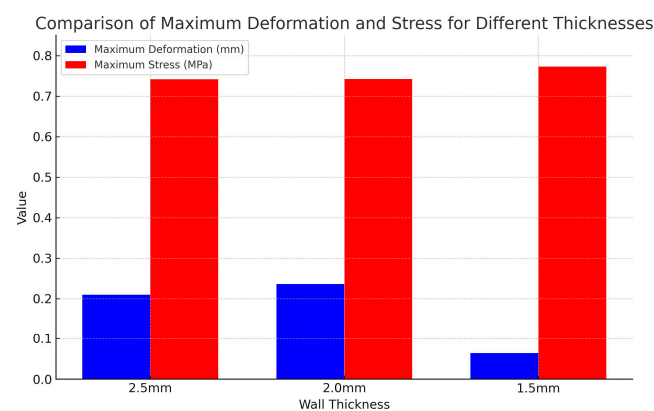


Figure 24. The total deformation and stress for the three thicknesses in the X+Y+Z direction.

Through an in-depth analysis of the simulation results for the three different thickness schemes, it is realized that selecting an appropriate thickness is crucial for optimizing the structural integrity of the box-type substation, while ensuring safety and durability. The 2.5 mm wall thickness may be more suitable for bearing loads in a single direction, but under the combined action of multiple directions, its stability is not as good as the 1.5 mm wall thickness. Although the deformation in a single direction is well controlled with a 2.0 mm wall thickness, the deformation is the largest in a combination of multiple directions, which increases the risk of structural failure in practical applications. The 1.5 mm wall thickness provides the best balance overall. Although the stress is slightly higher in individual directions, it maintains low deformation in all directions, especially under multi-directional combination effects. This illustrates the optimization of the design, making its structural design more reasonable. In structural design, control can avoid structural functional failure or premature fatigue. Therefore, the 1.5 mm wall thickness design demonstrated in simulation its advantages in maintaining structural integrity under the influence of comprehensive seismic waves, as well as its ability to maintain consistency and stability in all directions. This performance, taking into account structural safety and reliability, makes the 1.5 mm wall thickness a strong candidate. In summary, the combined simulation analysis of wind, snow, and seismic conditions not only enhances the understanding of the structural behavior of the box-type substation in this study but also highlights avenues for performance improvement through structural optimization.

5. Analysis of Selected Design Variants of the Considered Structure

5.1. Solution I: Adding Longitudinal Reinforcing Columns

Solution I involves mitigating stress concentration issues at specific points of the side wall panels by adding longitudinal reinforcement columns along the length direction of the wall.

These reinforcement columns are fixed to the inner or outer surfaces of the side wall panels, as depicted in Figure 25a. The material used is ST12, with a column diameter of 48 mm, and the height matches the total height of the box-type substation, which is 2102.5 mm.

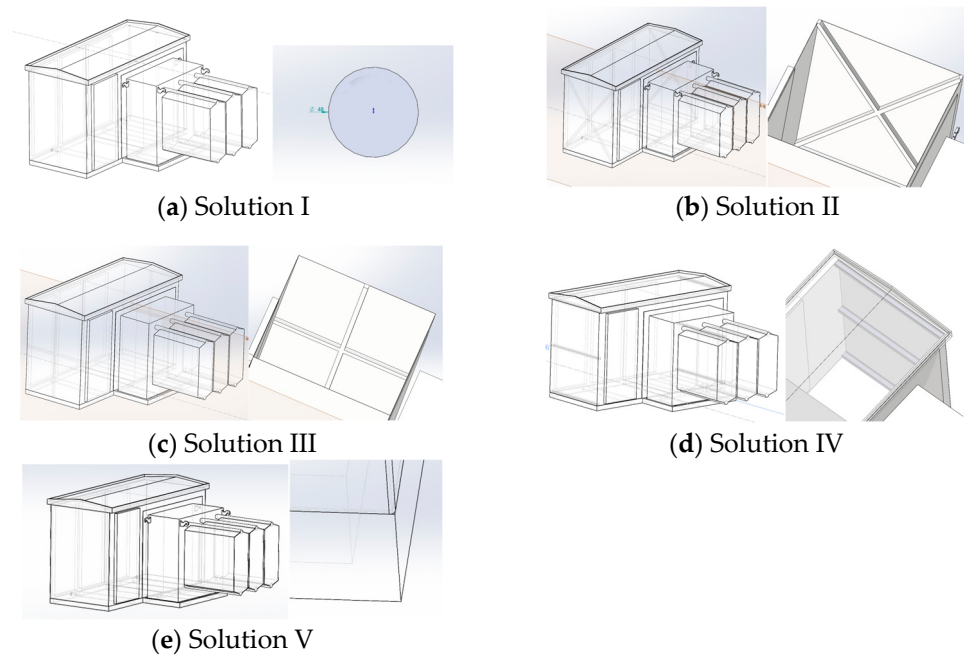


Figure 25. Model of Solutions I–IV.

Simulation results after adjusting the structure, as shown in Table 10, lead to the following conclusions:

1. **Deformation Analysis:** As the wall thickness decreases, there is a slight increase in deformation, indicating that thinner structures generally have a lower rigidity. The maximum deformation for all thicknesses primarily occurs in the Z and XZ directions, with the deformation in the Z direction being significantly larger compared to the X and Y directions.
2. **Stress Analysis:** The 2.0 mm-thickness side walls exhibit the lowest stress in the X direction, indicating that the reinforcement by columns is most effective for side walls of this thickness. In the Y direction, the stress values for the three different thicknesses do not vary significantly. However, in the Z direction, there is a slight increase in stress with a decreasing wall thickness, with the 1.5 mm-thickness side walls displaying the highest stress levels.

Table 10. Combination simulation results of three thicknesses under Solution I.

Thicknesses	Response	X	Y	Z	XZ	ZY
2.5 mm	Von Mises Stress (MPa)	0.52671	0.32637	4.0611	4.067	4.0611
	Total Deformation (mm)	0.051331	0.057588	1.1536	1.1547	1.1536
2.0 mm	Von Mises Stress (MPa)	0.22718	0.31417	4.1499	4.156	4.1499
	Total Deformation (mm)	0.052718	0.055495	1.1548	1.156	1.1548
1.5 mm	Von Mises Stress (MPa)	0.34629	0.32705	4.1478	4.1541	4.1478
	Total Deformation (mm)	0.054138	0.057823	1.1577	1.159	1.1577

In the simulation results after adjusting the structure, taking the 2.5 mm-thickness cloud map as an example (similar optimization levels are observed for the 2.0 mm and 1.5 mm maps), as shown in Figure 26, significant changes are evident: the phenomenon of deformation concentration in the side walls has been effectively alleviated, and stress concentration points at the junction of the side walls and brackets have been significantly

improved. This indicates that Solution I has achieved a significant effectiveness in enhancing structural stability and reducing stress concentrations.

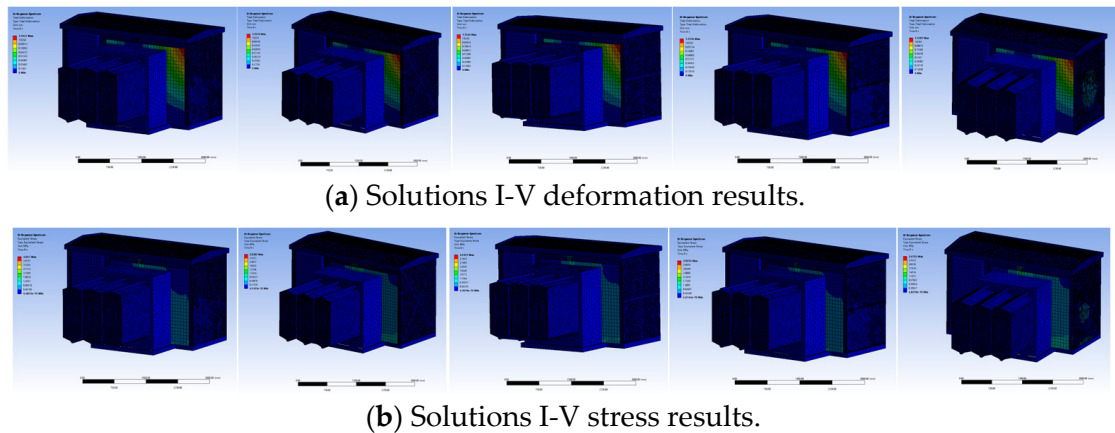


Figure 26. Solutions I-V simulation results.

5.2. Solution II: Cross-Bracing for Columns

Solution II introduces X-shaped steel bracing as a reinforcement measure, as depicted in Figure 25b. Using ST12 material, this scheme aims to resist deformation and stress under combined seismic and snow loadings by providing additional lateral support.

The simulation results are shown in Table 11, leading to the following conclusions:

1. **Deformation Analysis:** Across all wall thicknesses, the deformation of the side walls in the Y direction shows little variation, indicating relative rigidity in this direction. In the Z direction, the deformation in the 2.0 mm- and 1.5 mm-thickness side walls is slightly less than that of the 2.5 mm thickness, although the differences are minimal. This suggests that the reinforcement measures are also effective in resisting deformation in the Z direction.
2. **Stress Analysis:** For the 2.5 mm and 2.0 mm wall thicknesses, the maximum stress is primarily concentrated in the Z and XZ directions, indicating that external loads have the greatest impact in these directions. For the 1.5 mm-thickness side walls, the stress values are relatively lower in all directions, particularly in the Z direction, where the stress significantly reduces to 2.8339 MPa. This demonstrates that the X-shaped steel supports are more effective at dispersing stress in thinner wall panels.

Table 11. Combination simulation results of three thicknesses under Solution II.

Thicknesses	Response	X	Y	Z	XZ	ZY
2.5 mm	Von Mises Stress (MPa)	0.38186	0.41728	3.7005	3.7065	3.7005
	Total Deformation (mm)	0.052959	0.082141	1.1546	1.1558	1.1546
2.0 mm	Von Mises Stress (MPa)	0.30365	0.41812	3.923	3.9295	3.923
	Total Deformation (mm)	0.053293	0.082145	1.1496	1.1508	1.1496
1.5 mm	Von Mises Stress (MPa)	0.21748	0.41858	2.8339	2.8385	2.8339
	Total Deformation (mm)	0.055705	0.080392	1.1499	1.1512	1.1499

From the simulation results after adjusting the structure, the stress contour plot for the 2.5 mm-wall-thickness solution is shown in Figure 26, indicating a significant improvement in the previously observed deformation concentration on the side wall and the stress concentrations at the brace connections. The reinforcement measures of the X-shaped steel supports in Solution II have a significant effect in reducing stress and deformation in the Z direction; for side wall panels with a wall thickness of 1.5 mm, the improvement effect is most obvious.

5.3. Solution III: Cross-Shaped Steel Braces

Solution III employs cross-shaped steel bracing to enhance the structural stability of the box-type substation, utilizing ST12 material, as depicted in Figure 25c.

The simulation results, as shown in Table 12, lead to the following conclusions:

1. **Deformation Analysis:** The deformation in the Y direction shows little variation across all wall thicknesses, indicating the good overall rigidity of the structure in this direction. In the Z direction, despite the highest stress at the 1.5 mm thickness, its deformation is slightly lower than that of the 2.5 mm and 2.0 mm thicknesses. This suggests that, despite the higher stress, the cross-shaped steel supports still help to control the deformation of the thinner wall panels to some extent.
2. **Stress Analysis:** Across all thicknesses, the stress in the Z direction increases as the wall thickness decreases. The 2.5 mm thickness exhibits the lowest stress, while the 1.5 mm thickness shows the highest stress. This suggests that the cross-shaped steel supports are less effective at countering stress in the Z direction for thinner walls. The stress variations in the X and Y directions are minimal, indicating that the reinforcement effect of the cross-shaped steel supports is relatively uniform across these directions.

Table 12. Combination simulation results of three thicknesses under Solution III.

Thicknesses	Response	X	Y	Z	XZ	ZY
2.5 mm	Von Mises Stress (MPa)	0.39249	0.3623	3.5288	3.5351	3.5288
	Total Deformation (mm)	0.053931	0.067546	1.1509	1.1522	1.1509
2.0 mm	Von Mises Stress (MPa)	0.33654	0.36237	3.8212	3.8276	3.8212
	Total Deformation (mm)	0.05526	0.067625	1.1515	1.1529	1.1515
1.5 mm	Von Mises Stress (MPa)	0.24349	0.36263	3.9997	4.0073	3.9997
	Total Deformation (mm)	0.054887	0.067747	1.1441	1.1454	1.1441

From the simulation results after adjusting the structure, the stress contour plot for the 2.5 mm-thickness scheme is shown in Figure 26, revealing a significant alleviation of the deformation concentration phenomenon previously observed in the side panels, and a noticeable reduction in stress concentration points at the junction of the side panels and supports. Similar to the stress contour plots for the 2.0 mm- and 1.5 mm-thickness schemes, this demonstrates the universal applicability and effectiveness of the cross-shaped steel bracing solution across box-type substation structures with different thicknesses.

5.4. Solution IV: H-Beam Bracing

Solution IV involves adding horizontal H-shaped steel sections to the upper and lower edges of the side panels, as depicted in Figure 25d. The material selected is ST12, with the assumption that the box-type substation design incorporates four support beams to share the load, with each beam bearing approximately 30825 N of load. Due to structural constraints within the box, the beam width is limited to a maximum of 48 mm. Calculations yield the dimensions of the H-shaped steel as follows: length 1500 mm (equivalent to the length of the side panels), width 48 mm, and height 10.9 mm.

The simulation results after adjusting the structure are shown in Table 13, leading to the following conclusions:

1. **Deformation Analysis:** The deformation is greatest in the 1.5 mm thickness, indicating that the support from the H-shaped steel is slightly less effective for thinner walls. The deformation in the X and Y directions is relatively consistent across all thicknesses, demonstrating that the H-shaped steel provides adequate lateral support, maintaining the overall rigidity of the structure.
2. **Stress Analysis:** In all thicknesses, the stress in the Z direction increases as the wall thickness decreases, with the 1.5 mm thickness showing the highest stress, indicating that the structural load-bearing capacity decreases with a reduced wall thickness. The

2.5 mm thickness exhibits higher stress in the X direction, while in comparison, the stress significantly decreases in the 2.0 mm thickness (0.23713 MPa), demonstrating that the H-shaped steel reinforcement is more effective for medium wall thicknesses.

Table 13. Combination simulation results of three thicknesses under Solution IV.

Thicknesses	Response	X	Y	Z	XZ	ZY
2.5 mm	Von Mises Stress (MPa)	0.5293	0.3024	3.8951	3.9014	3.8951
	Total Deformation (mm)	0.054082	0.054972	1.1523	1.1536	1.1523
2.0 mm	Von Mises Stress (MPa)	0.23713	0.30283	3.9926	3.9992	3.9926
	Total Deformation (mm)	0.055864	0.055014	1.1532	1.1545	1.1532
1.5 mm	Von Mises Stress (MPa)	0.72434	0.30298	4.007	4.0136	4.007
	Total Deformation (mm)	0.056786	0.055097	1.1553	1.1567	1.1553

The simulation contour plot, as depicted in Figure 25e illustrates that the addition of H-shaped steel reinforcement components along the upper and lower edges of the side panels has enhanced the rigidity and stability of the box-type substation structure, reducing the deformation caused by external forces.

5.5. Solution V: Fillet

Solution V optimizes structural details by designing fillets at the connection between the side wall panel and the support, aiming to reduce the stress concentration caused by sharp angles. The fillet radius is set to 5 mm, as shown in Figure 25e.

The simulation results after adjusting the structure, as shown in Table 14, lead to the following conclusions:

1. Deformation Analysis: In the Z direction, as the wall thickness decreases, the amount of deformation gradually increases, particularly in the 1.5 mm thickness, where the deformation is the greatest. This indicates that, while the rounded corner design aids in controlling deformation to some extent, its effectiveness is limited for thinner wall thicknesses.
2. Stress Analysis: The 2.5 mm thickness exhibits relatively low stress in the Z direction, indicating that the rounded corner design effectively reduces stress concentrations in thicker wall thicknesses. The stress in the Z direction significantly increases for the 2.0 mm thickness, suggesting that the rounded corner design does not sufficiently alleviate stress concentrations in medium thicknesses. The 1.5 mm thickness shows the highest stress in the Z direction (6.7582 MPa), indicating that, despite the rounded corner design, stress concentration remains a significant issue in the thinnest wall thickness.

Table 14. Combination simulation results of three thicknesses under Solution V.

Thicknesses	Response	X	Y	Z	XZ	ZY
2.5 mm	Von Mises Stress (MPa)	0.75156	0.36199	2.6087	2.6124	2.6087
	Total Deformation (mm)	0.2321	0.067577	1.1568	1.1581	1.1568
2.0 mm	Von Mises Stress (MPa)	1.7812	0.022959	5.3453	5.3549	5.3453
	Total Deformation (mm)	0.28641	0.0021908	1.1803	1.1817	1.1803
1.5 mm	Von Mises Stress (MPa)	0.68539	0.0049452	6.7582	6.7717	6.7582
	Total Deformation (mm)	0.29483	0.001683	1.1615	1.1628	1.1615

Solution V, as a structural detail optimization measure, plays a certain positive role in enhancing the stability of the box-type substation structure and reducing stress concentrations. However, as the thickness decreases, the effectiveness of the optimization in controlling the maximum deformation and stress gradually diminishes.

The simulation analysis of various structural optimization solutions for box-type substations highlights key insights into enhancing structural stability and reducing stress

concentration. Although all solutions aim to enhance structural stability and reduce stress concentrations, their effectiveness varies depending on the wall thickness and the specific directional stresses they address. Specifically, Solution I significantly improves stability and reduces stress concentrations in thicker walls, particularly effectively in the Z and XZ directions. Solutions II and III are especially effective in reducing stress and controlling deformation in thinner walls. However, they exhibit limitations in thicker walls, where stress concentration remains an issue despite reinforcement. Solution V, while innovative in addressing stress points at sharp angles, shows limitations in thinner walls, indicating that, although it can reduce stress concentrations, it does not significantly impact the overall stress levels in critical areas. Meanwhile, Solution IV demonstrates a strong ability to enhance rigidity and reduce stress across different wall thicknesses, particularly at a medium thickness, where it significantly lowers stress in the X direction.

5.6. Comprehensive Analysis

5.6.1. Simulation Comparison for Different Thicknesses under Each Solution

First, an analysis is conducted on the simulation results of three different side wall thicknesses under various solutions for the box-type substation, as shown in Figure 27a–c.

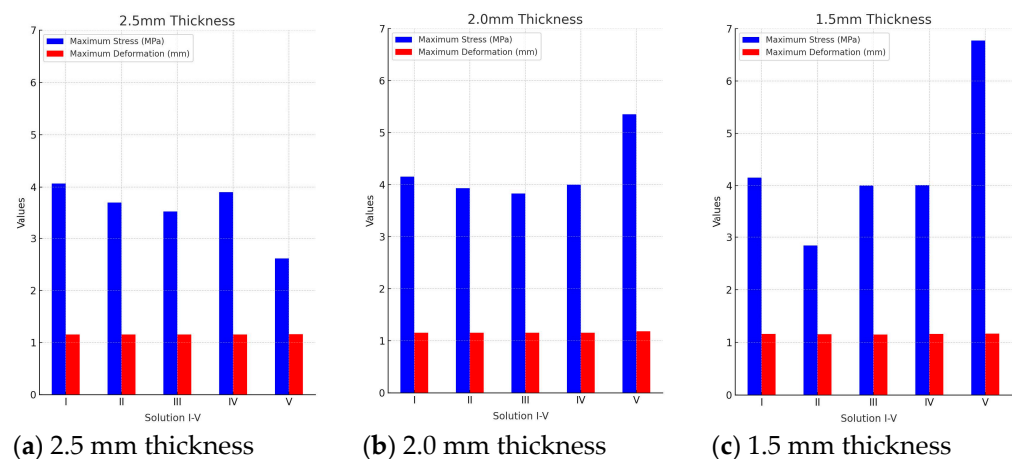


Figure 27. Comparison of different thicknesses of wall panels under each solution.

An analysis of the simulation results for three different thicknesses of wall panels under various solutions reveals the following:

1. **Deformation Analysis:** As the thickness decreases, the maximum deformation generally increases, although the trend is not significant. Notably, Solution V exhibits the highest deformation values in thinner walls, particularly at the 2.0 mm and 1.5 mm thicknesses. In contrast, Solutions II and III demonstrate smaller deformations across most thickness conditions, suggesting that these schemes may offer better structural strength and durability.
2. **Stress Analysis:** In all solutions, as the thickness of the side walls decreases, the maximum stress values increase. This indicates that thinner materials endure higher stresses under the same loading conditions, increasing the risk of material failure. Notably, Solution V exhibits the highest stress values across all thicknesses, especially at 2.0 mm and 1.5 mm, suggesting that this scenario places the most demanding stress requirements on the materials. In contrast, Solutions II and III generally show lower stress levels across most thicknesses, potentially indicating more robust design choices.

5.6.2. Simulation Comparison of Different Solutions at Various Thicknesses

Next, an analysis of the comparative performance of the stress and deformation results for the five solutions across three thicknesses is presented in Figure 28.

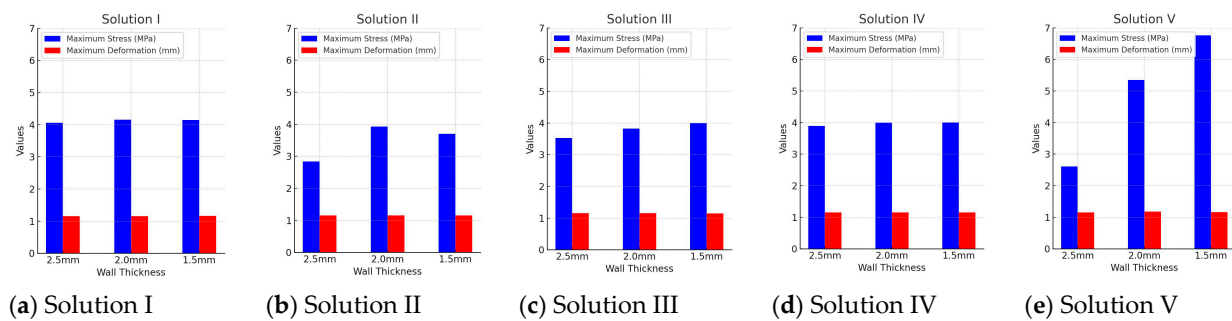


Figure 28. The stress and deformation results of the five solutions are compared under three different wall thicknesses.

From Figure 28a–e, it can be observed that:

1. **Deformation Analysis:** Among these five solutions, the deformation changes are relatively stable as the wall thickness varies. Notably, Solution III exhibits the lowest deformation values, ranging from 1.1441 to 1.1522 mm, demonstrating excellent deformation control performance.
2. **Stress Analysis:** Solution I demonstrates good structural robustness, with relatively stable stress values across all thickness levels. In contrast, Solution II exhibits reduced stress values at thinner thicknesses, ranging from 2.8339 MPa at 1.5 mm to 3.923 MPa at 2.0 mm, indicating decreased structural stability as the material thins. Solution III maintains consistently low stress values, between 3.5288 and 3.9997 MPa across all thicknesses, suggesting a balanced stress resistance. Solution IV shows a similarly stable stress performance, with stress values ranging from 3.8951 to 4.007 MPa. Conversely, Solution V reveals a significant dependency on thickness, with stress levels sharply increasing from 2.6087 MPa at 2.5 mm to 6.7582 MPa at 1.5 mm, highlighting potential issues with high stress in thin-wall conditions.

To determine the optimal solution and thickness, considering the data from both sets of charts, the following conclusions are drawn:

1. Considering the analysis of stress and deformation characteristics at different thicknesses, Solution III is shown to be the most stable choice among the five options. It provides a robust balance between stress resistance and deformation control. It exhibits the lowest deformation values at various thicknesses. Although other schemes also show relatively stable deformations with changes in wall thickness, Solution III has a clear advantage. This advantage is crucial for maintaining the integrity of the structure under various loads and conditions.
2. Although thicker side walls (2.5 mm) generally offer better structural performance, with smaller deformations and stress, at a thickness of 2.0 mm, although the stress increases compared to 2.5 mm, the increase is more moderate compared to 1.5 mm, and the performance is similar to 2.5 mm. This suggests that a thickness of 2.0 mm may be a reasonable compromise in terms of cost-effectiveness and material efficiency.
3. While Solution V performs well at thicker dimensions, it exhibits a significant increase in stress as the material becomes thinner; therefore, this solution is ruled out.

The comparison of the results before and after the structure and wall thickness adjustments is shown in Table 15. Before adjusting the structure, there was a stress concentration in the side wall panels. After adjusting the structure, this phenomenon was eliminated, and the strength and stability of the structure were ensured through simulation.

Table 15. Comparison of simulation values before and after adjustment.

Thicknesses	2.5 mm (before)	2.0 mm (after)
Von Mises Stress (MPa)	0.74187	3.8276
Total Deformation (mm)	0.20958	1.1529
Side wall panel quality (Kg)	117	98.0928

6. Conclusions

Through an analysis of potential seismic hazard scenarios and combined wind and snow loads, appropriate boundary conditions were established based on the load forms and magnitudes experienced by the box-type substation enclosure under these conditions. These boundary conditions were set to maximize the fidelity of the enclosure's representation. Utilizing finite element analysis (FEA) methods, an assessment of the enclosure's structural strength and stiffness was conducted, accompanied by a simplification of the experimental procedures. This approach theoretically enhanced the accuracy of the enclosure simulation and was validated through parametric simulation studies. The conclusions are as follows:

1. After a comparative analysis of five plans, this study found that reducing the thickness by 0.5 mm to achieve a thickness of 2.0 mm lowers material usage costs. By employing a cross-bracing structure on the side walls, the structural strength and stiffness are maintained. Specifically, the mass of the side wall panels was reduced from 117 kg to 98.0928 kg, resulting in a weight reduction of 18.9072 kg. This reduction not only demonstrates a decrease in material costs but also ensures that the structural integrity is not compromised, thanks to the added cross-bracing. This finding is significant for enhancing the design efficiency of box-type substation enclosures, as it provides a practical approach to achieving cost-effectiveness, while maintaining necessary structural properties.
2. Compared to the original model, the improved box-type substation enclosure exhibits a deformation and maximum equivalent stress within the range of structural strength, reducing stress concentration phenomena and enhancing the enclosure's resistance to deformation. This ensures its normal operation under extreme conditions and prevents fracture occurrences.
3. Through a detailed simulation analysis, a deeper understanding of the specific effects of different optimization solutions on the performance of the box-type substation enclosure has been achieved, providing a more scientific basis for the structural design and material selection. Particularly in considering the potential impacts of thickness reduction on structural performance, this study offers an effective approach towards achieving lightweight enclosure structures with optimized performance.

In summarizing our findings, it is necessary to reflect on the static methods used to simulate wind and snow loads. This approach proved effective within the specific range of our study, providing a solid starting point for evaluating structural response under maximum loads. It allows us to simplify our focus, allowing us to gain initial insights within the resource and time constraints typical of early design evaluations. However, we recognize the inherent limitations of static analysis—in particular, its inability to account for the complex interplay of time-dependent loading effects that are characteristic of dynamic environmental forces, such as wind gusts or heavy snowfall that accumulates over time. As we advance, it becomes critical to explore dynamic modeling that incorporates time-varying loads, to more accurately capture the subtle behavior of the structure under such conditions.

Therefore, future research should provide a more comprehensive understanding of the load response by integrating dynamic analysis methods. This may involve transient simulations that reflect the fluctuating nature of environmental forces or experimental verification that validates computational predictions. Additionally, the practical implications of adopting one analytical method over another must be carefully considered, balancing accuracy against cost, the practicality of the available technology, and project timelines.

To align our research with these future directions, we intend not only to expand the scope of the study but also to enhance its applicability to real engineering problems. Through this discussion, we aim to make a constructive contribution to the body of knowledge and encourage further research into the dynamic aspects of structural load analysis.

Author Contributions: Conceptualization, M.G.; methodology, M.G.; software, M.G.; validation, M.F. and L.W.; writing—review and editing, M.G.; visualization, J.H. and J.Q.; supervision, J.H. and J.Q. All authors have read and agreed to the published version of the manuscript.

Funding: This research is supported by the National Key R&D Program of China (2022YFB3402001), National Natural Science Foundation of China (52035007, U23B20102).

Institutional Review Board Statement: Not applicable.

Informed Consent Statement: Not applicable.

Data Availability Statement: The data reported in this study can be found in the sources cited in the reference list.

Conflicts of Interest: The authors declare no conflicts of interest.

References

1. Wang, N. Research on Electromagnetic and Thermal Issues of Box Type Substation. Master's Thesis, Shenyang University of Technology, Shenyang, China, 2019.
2. Zhou, X. Research on Seismic Action Analysis of Steel Frame Structures Based on ANSYS. Master's Thesis, Hebei University of Engineering, Handan, China, 2014.
3. Yu, J.; Yu, J. Brief analysis of the typhoon resistance capability of box type substations. *Transformer* **2021**, *58*, 11–14.
4. Zhou, X.; Gu, M.; Li, G. Grouping response method for equivalent static wind loads based on a modified LRC method. *Earthq. Eng. Eng. Vib.* **2012**, *11*, 107–119. [[CrossRef](#)]
5. Chen, Y.; Dai, B.; Zhou, Y. Stress Analysis Method of 110kV Prefabricated Substation Box Based on Finite Element Principle. In *Internet of Things and New Electric Power Technologies—Proceedings of the 2014 Yunnan Electric Power Technology Forum*; Yunnan Power Grid Co., Ltd.: Kunming, China; Yunnan Electrical Engineering Society: Kunming, China; Yunnan Science and Technology Press: Kunming, China, 2014; Volume 1.
6. Jiang, J.; Geng, G.; Li, J.; Wang, J.; Shang, W.C.; Zhang, H.Q.; Zhang, S.C. A Vertical Box Shock-Absorbing Substation. Shandong Province. CN112186580B, 2 September 2022.
7. Tuerker, T.; Bayraktar, A. Finite element model calibration of steel frame buildings with and without brace. *J. Constr. Steel Res.* **2013**, *90*, 164–173. [[CrossRef](#)]
8. Aiello, G.; Vaccaro, A.; Combescure, D.; Gessner, R.; Grossetti, G.; Meier, A.; Saibene, G.; Scherer, T.; Schreck, S.; Spaeh, P.; et al. The ITER EC H&CD Upper Launcher: Seismic analysis. *Fusion Eng. Des.* **2014**, *89*, 1809–1813.
9. Gupta, A.K. *Response Spectrum Method in Seismic Analysis and Design of Structures*; Routledge: London, UK, 2017.
10. GB 50260-2013; Code for Seismic Design of Electric Power Facilities. China Power Engineering Consulting Group Northwest Electric Power Design Institute: Xi'an, China, 2013.
11. *Release 11.0. 2007*; ANSYS Incorporated. Programmer's Manual for ANSYS. ANSYS: Pittsburgh, PA, USA, 2007.
12. Wang, T.; Huang, Z.; Ding, J.; Xu, G.; Gu, W.; Zhang, D. 220 kV indoor substation roof frame structure system and its seismic performance. *Electr. Power Eng. Technol.* **2017**, *36*, 76–80+92.
13. Cai, X.; Zhao, Y.; Wei, Z.; Chang, L.C. Calculation Method of Strain Distribution of Bi-directional Curvature Plate Based on Subroutine Secondary Development. *Chin. J. Ship Res.* **2022**, *17*, 212–219.
14. Qin, Q. Fatigue Performance Analysis of Multi-spot Welded Joints of ST12 Steel. Master's Thesis, Kunming University of Science and Technology, Kunming, China, 2022.
15. Lee, S.E.; Lee, D.M. Development of Numerical Modelling Techniques for a Firefighting Water Tank with an Anti-Wave Plate under Seismic Loads. *Appl. Sci.* **2023**, *13*, 11689. [[CrossRef](#)]
16. Zhao, G.Y.; Fu, P.; Zhou, S.W. Dynamic mechanical analysis of automotive gearbox casing. *Adv. Mater. Res.* **2011**, *230–232*, 539–543. [[CrossRef](#)]
17. Liang, C.; Zhu, L. A case study on dome structure of composite structural insulation panels with ANSYS simulations. *Front. Mater.* **2022**, *9*, 1072600. [[CrossRef](#)]
18. Avitabile, P. Experimental modal analysis. *Sound Vib.* **2001**, *35*, 20–31.

19. Xia, T. 110kV GIS Seismic Simulation and Optimization Based on Finite Element. Master's Thesis, Xiamen University of Technology, Xiamen, China, 2016.
20. GB 18306-2001; Earthquake Motion Parameter Zoning Map of China. Standardization Administration of China: Beijing, China, 2001.

Disclaimer/Publisher's Note: The statements, opinions and data contained in all publications are solely those of the individual author(s) and contributor(s) and not of MDPI and/or the editor(s). MDPI and/or the editor(s) disclaim responsibility for any injury to people or property resulting from any ideas, methods, instructions or products referred to in the content.